# Formation and Decomposition of High-mass Metal–Oxygen Cluster Ions in the Fast Atom Bombardment of Lanthanide Salts

**Terence J. Kemp* and Paul A. Read**
*Department of Chemistry, University of Warwick, Coventry CV4 7AL, UK*

Fast atom bombardment of lanthanide nitrates in involatile organic matrices gave rise to series of lanthanide–oxygen cluster monocations of general formula $[(LnO)_xO_y]^+$ containing up to 40 metal atoms, *e.g.* $[(LaO)_{33}O_{19}]^+$, $[(HoO)_{27}O_{14}]^+$ and $[(PrO)_{41}O_{20}]^+$. The behaviour within each series depends on the metal atom, but odd–even alternation effects in the ion abundances are universal, with some even-$x$ members missing altogether. The stoichiometry of the clusters also depends on the metal atom, with virtually all series displaying regions of particular stoichiometry, the ratio $y:x$ increasing sharply at particular $x$ values. These well defined regions are particularly numerous for lanthanides (Eu and Sm) featuring two relatively stable oxidation states. There also appear to be certain 'islands of stability' where a particular value of $x$ is associated with exceptional stability. Collision-induced decomposition studies of a variety of the cluster ions revealed loss of LnO, $LnO_2$ or $Ln_2O_3$ moieties, with relative abundances of daughter ions dependent on the pressure of the collision gas; odd–even alternation effects were again observed. Consideration of the detailed stoichiometry of the cluster ions suggests remarkable parallels with the phase behaviour of the lanthanide oxides in the solid state.

The tendency towards clustering in the gas phase has been noted for a number of inorganic and organometallic compounds[1] since the development of fast atom bombardment (FAB) mass spectrometry in 1981.[2] We have given some key references in an earlier paper,[3] but would draw attention here to the work of Selbin and co-workers[4] who found FAB of Schiff bases and simple salts of 12 lanthanides to give a series of positive cluster ions of general formula $[(LnO)_xO_y]^+$ containing up to nine Ln atoms. A later paper by Selbin and co-workers[5] reported collisionally induced decomposition (CID) of yttrium oxide cluster ions to give, as the most abundant ions, $[Y_aO_{(3a-1)/2}]^+$ where $a$ is an odd number (*e.g.* $[YO]^+$, $[Y_3O_4]^+$, $[Y_5O_7]^+$ and $[Y_7O_{10}]^+$). Thus $[Y_7O_{10}]^+$ decomposes to give principally $[Y_3O_4]^+$ (85), $[Y_5O_7]^+$ (7), $[Y_7O_{10}]^+$ (100%) with minor amounts of $[Y_4O_6]^+$ (11) and $[Y_6O_8]^+$ (7%).

Extensive series of metal–oxygen cluster ions have also been produced by other means and identified mass spectrometrically. Sputtering of metal foils followed by reaction with oxygen yields series[6] such as $[TiO(TiO_2)_{x-1}]^+$, while reaction of iron clusters with oxygen yields product ions $[Fe_xO_x]^+$ when $3 \leqslant x \leqslant 9$, $[Fe_xO_{x+1}]^+$ when $10 \leqslant x \leqslant 13$, $[Fe_xO_{x+2}]^+$ when $14 \leqslant x \leqslant 22$ and $[Fe_xO_{x+3}]^+$ when $23 \leqslant x \leqslant 31$; the 'iron deficiency' reaches six in $[Fe_{59}O_{65}]^+$. Another study[7] reported $[Fe_xO_2]^+$ $(2 < x < 18)$ and $[Fe_xS]^+$ in reactions of $Fe_x$ with $O_2$ and $H_2S$.

Electrospray mass spectrometric examination of β-diketone ($H_2L$) complexes of lanthanide ions (Eu, Yb or Gd) revealed ligand exchange[8,9] (involving 1% acetic acid in the MeOH–water solution) and the formation of small clusters,[8] *e.g.* $[Eu_2(H_2L)_2(O_2CMe)_3]^+$ and $[Gd_2(H_2L)_2(O_2CMe)_3]^+$ ($H_2L$ = 2,2,6,6-tetramethylheptane-3,5-dione).

In the present study we used a high-mass tandem mass spectrometer to extend the range of accessible lanthanide clusters to species containing over 40 metal atoms and to investigate much longer CID sequences than has been possible hitherto.

## Experimental

Experiments were carried out using a Kratos Analytical Ltd. 'Concept' four-sector mass spectrometer as described before.[3] Collisionally induced decomposition experiments were carried out using a Flexicell as described before,[3] with argon as the collision gas and the cell maintained at a potential of 2 kV.

As most experiments involved very large mass ranges, the Concept spectrometer was not calibrated for each mass region on every occasion. Accordingly, the $m/z$ ratios recorded in Figures and Tables are sometimes slightly out of calibration (by the order of a few units in several thousand). Accurate calibrations *were* carried out over the full mass range for all lanthanides to verify the assignments made: the spectra chosen for inclusion are those thought to be most complete or illustrative.

Lanthanide nitrates and acetates were used as supplied by Aldrich and BDH, as was the principal organic matrix material, sulfolane (tetrahydrothiophene 1,1-dioxide).

## Results

*Lanthanum–Oxygen Clusters.*—The FAB spectrum of lanthanum nitrate in a sulfolane matrix is shown in Fig. 1. The peaks correspond to the general formula $[(LaO)_xO_y]^+$ as first reported by Selbin and co-workers.[4] The series based on $[(LaO)O_y]^+$ is much the most intense, and $y$ varies from 1 to 5. The abundance falls off exponentially as $x$ increases. While the species $[(LaO)_2O]^+$ is relatively abundant, a very strong alternation effect appears at $x \geqslant 3$, with the odd-$x$ species completely dominating the spectrum. This mirrors the alternation reported by Selbin and co-workers[4] for the yttrium–oxygen series.

In the di- and tri-lanthanum series the species with a value of $y$ of 1 is much the most abundant; when $x = 4$ and 5 then the $y = 2$ species dominates. This pattern is developed as $x$ increases up to 9, and the most intense species in each group (*i.e.* given value of $x$) corresponds to a mass difference of a $(LaO)_2O$ unit. At values of $x > 9$ the even-$x$ clusters become very low in abundance until at $x = 12$ they disappear altogether. As regards the odd-$x$ series, the most abundant members at each value of $x$ are again separated by a mass difference equivalent to $(LaO)_2O$. This behaviour continues right up to $x = 25$.

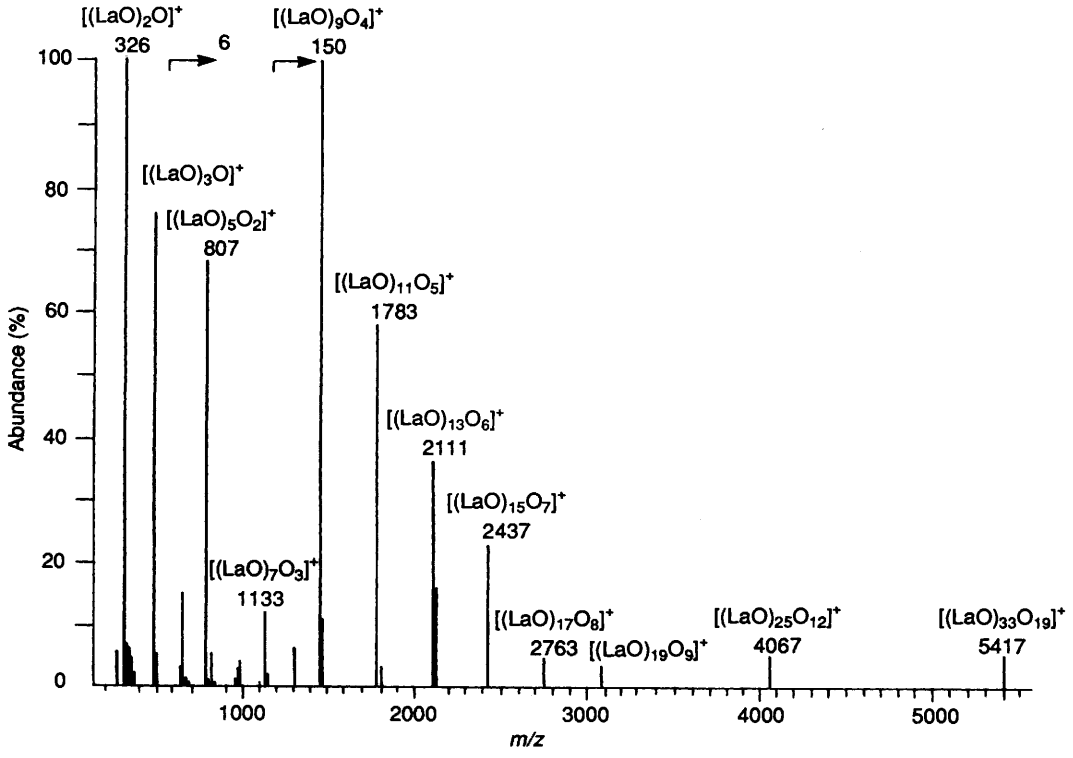


**Fig. 1** The FAB spectrum of lanthanum nitrate in a sulfolane matrix. Numbers above arrows refer to scaling-up factors

**Table 1** Ranges of $x$ and $y$ in the series of clusters $[(LaO)_xO_y]^+$ for odd values of $x$

| Range in $x$ | Increase in $y$ between successive members | Unit added |
|---|---|---|
| 1–9 | 0 or 1 | LaO or $(LaO)_2O$ |
| 9–25 | 1 | $(LaO)_2O$ |
| 25–27 | 3 | $(LaO)_2O_3$ |
| 27–33 | 4 | $(LaO)_6O_4$ |

For clusters with $x > 25$ the next detectable species was $[(LaO)_{27}O_{15}]^+$ ($m/z = 4423$), corresponding to addition of $(LaO)_2O_3$ to the most abundant species in the $x = 25$ series. No species with $x = 29$ or 31 was detectable but $[(LaO)_{33}O_{19}]^+$ at $m/z = 5419$ was much more intense than the $x = 27$ species and comparable with the abundances of the $x = 17$, 19 and 25 species, indicating the existence of a so-called 'magic number'.

*Lanthanum–Oxygen Cluster Stoichiometries.*—Even -$x$ clusters display a $y:x$ ratio of 0.5:1. Their intensities fall off rapidly as $x$ increases until at $x > 9$ their abundance is essentially zero. Cluster ions with odd values of $x$ show a set of discernible regions of stoichiometry as summarised in Table 1. The first region ($x = 1$–9) features the steady addition of $(LaO)_2O$ units between successive members of the odd-$x$ series. In the next series ($x = 9$–25) the mass differences between adjacent clusters corresponds to $(LaO)_2O$ units and we find a $y:x$ ratio of 0.44–0.48:1. Between $x = 25$ and 27 the addition of $(LaO)_2O_3$ units leads to a sharp increase in the $y:x$ ratio from 0.48 ($x = 25$) to 0.55:1 ($x = 27$). This observation, together with the unexpected appearance of a strong peak at $x = 33$, implies (*i*) that the clusters are not simply aggregates of $La^{3+}$ and $O^{2-}$ ions with peaks at any combination of ions leaving a net charge of +1 and (*ii*) that the sharp changes in stoichiometry are associated with the development of new electronic structures at particular values of $x$.

Of interest also is the detection of a series of less-abundant clusters in the size range $x = 9$–18: these also had a general formula $[(LaO)_xO_y]^+$ but with an $y:x$ ratio of approximately 0.125:1.

$$[(LaO)_xO_y]^+ \xrightarrow{-(LaO)O} [(LaO)_{x-1}O_{y-1}]^+ \xrightarrow{-LaO} [(LaO)_{x-2}O_{y-1}]^+ \quad (1)$$

($x$ odd) ($x$ even) ($x$ odd)

*e.g.*

$$[(LaO)_{10}O_5]^+ \xrightarrow{-LaO_2} [(LaO)_9O_4] \xrightarrow{-LaO_2} [(LaO)_8O_3]^+ \xrightarrow{-LaO} [(LaO)_7O_3]^+ \xrightarrow{-LaO} [(LaO)_6O_3]^+ \xrightarrow{-LaO_2} [(LaO)_5O_2] \quad (2)$$

**Scheme 1**

*Collision-induced Decomposition (CID) of Lanthanum–Oxygen Clusters.*—These were carried out using argon and xenon at a variety of pressures, with the Flexicell being maintained at a potential of 2 kV. All spectra showed the same basic fragmentation pattern, *i.e.* only clusters with odd values of $x$ are at all abundant, species with even $x$ values being of very low intensity or even totally absent (see, for example, Fig. 2).

The principal peaks of the spectra are separated by 326 Daltons, *i.e.* corresponding to the sequential loss of $(LaO)_2O$ units between successive daughter clusters of odd $x$ value. However, we did note that the presence (albeit to a lesser degree) of clusters with even values of $x$ depended on the pressure of the collision gas, implying that two smaller neutral species are lost in sequence rather than as a single dimer unit, $(LaO)_2O$. The sequence normally takes the form in Scheme 1. The overall situation can be represented as in Scheme 2.

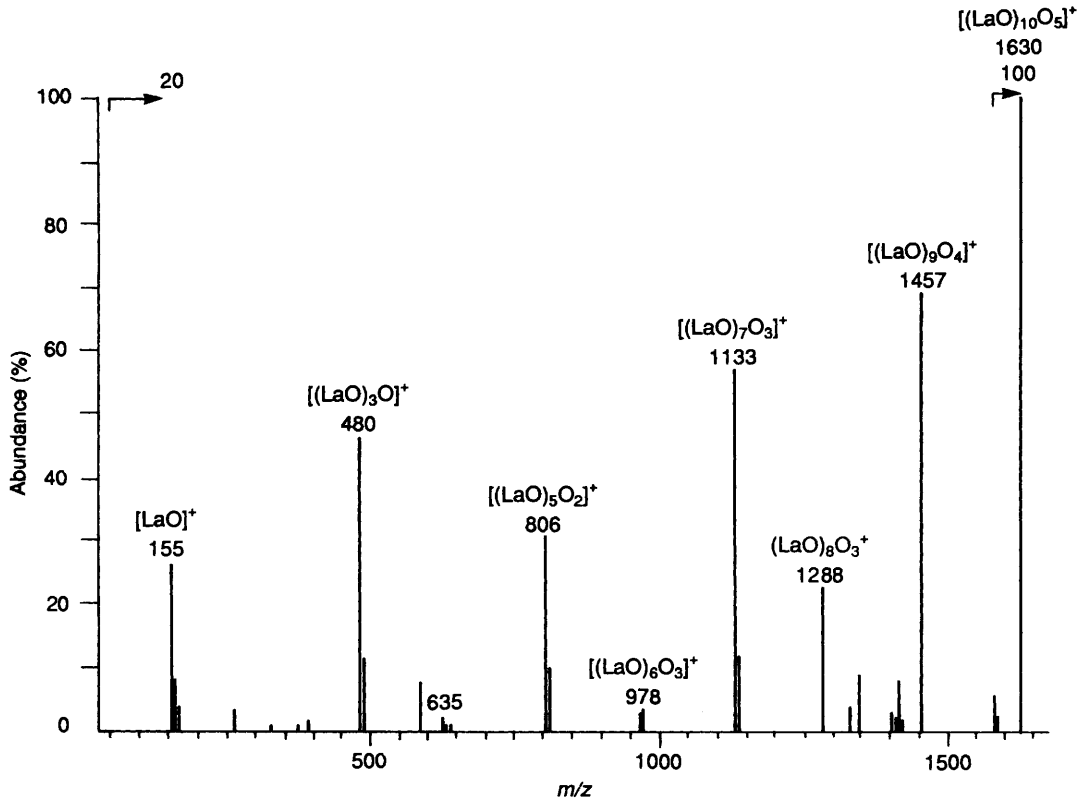


**Fig. 2** The CID spectrum of $[(LaO)_{10}O_5]^+$ ion

**Table 2** Stoichiometric behaviour of $[(CeO)_xO_y]^+$ clusters in FAB of cerium nitrate

| $x$ | $y$ |
|---|---|
| 1 | Extends from 0 to 6 with $[CeO]^+$ ($m/z$ = 156) dominating under all conditions (matrix, *etc.*) |
| 2, 3 | $[(CeO)_xO]^+$ species dominant (see peaks at $m/z$ = 328 and 484 respectively in Fig. 3) |
| 4, 5 | $[(CeO)_xO_2]^+$ species dominant |
| 6 | $[(CeO)_6O_3]^+$ dominant |
| 7 | $[(CeO)_7O_3]^+$ (calc. $m/z$ 1140) and $[(CeO)_7O_4]^+$ ($m/z$ = 1172) dominant |
| 8 | $[(CeO)_8O_y]^+$ with $y$ = 3, 6 or 7 dominant |
| 9 | Covers full range 0–9 with $y$ = 8 dominant and $y$ = 4 strong |
| 10–14 | Values of dominant species increase as $x$ increases |
| 15 | Discontinuity occurs: intense peaks found at much reduced $y$, *e.g.* at 2, 3, 7 and also 13, 14 |
| 15–21 | Three series of values identified at $x$ = 15 continues, with $y$ in each series gradually increasing with $x$. Slight odd–even alternation |
| >21 | Cluster intensity pattern irreproducible |
| 26 | $[(CeO)_{26}O_{10}]^+$ and $[(CeO)_{26}O_{11}]^+$ identified |

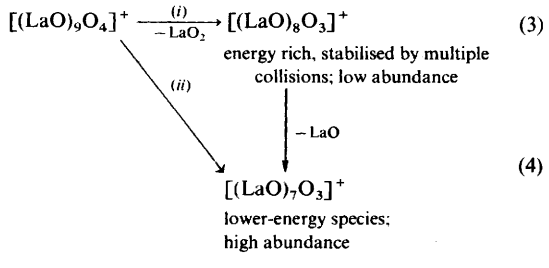


**Scheme 2** (*i*) High pressure of collision gas; (*ii*) all pressures of collision gas

*Stoichiometries of FAB- and CID-derived Lanthanum–Oxygen Species.*—In both sets of spectra we find (*i*) that species with odd values of $x$ are much more highly abundant (and therefore stable) than the corresponding species with even values of $x$ and (*ii*) that the $y$:$x$ ratio changes sharply at $x$ > 25. Also a magic number appears at $x$ = 33 in the FAB spectrum.

*Cerium–Oxygen clusters.* As with lanthanum, the general formula of any cluster detected is $[(CeO)_xO_y]^+$. Unlike the situation with lanthanum, clusters with even and odd values of $x$ were detected over the complete range of $x$ examined, *i.e.* up to $x$ = 26. With each value of $x$ there exists a range of $y$ values, but the extent of this range diminished as $x$ was increased. The fall off in abundance as $x$ is increased is readily apparent from Fig. 3 which covers the range only from $x$ = 1 to 9. Comments concerning individual sets of clusters are set out in Table 2.

A graphical representation of the $y$ values of the most-abundant species from each sequence *versus* the corresponding value of $x$, shown in Fig. 4, indicates a set of linear relationships between $x$ and $y$.

*Praseodymium–Oxygen clusters.* Species $[(PrO)_xO_y]^+$ are found with $x$ reaching 41, and the principal spectral feature is the strong odd–even alternation effect with even-$x$ species being much less abundant and decreasing to very low levels at $x$ > 31 (Fig. 5). In all spectra the base peak was $[PrO]^+$ ($m/z$ 157) with $[(PrO)O_4]^+$ also very visible in all matrices. The matrix had a significant effect on the abundances, with dimethyl sulfoxide giving much greater yields of high-mass clusters than did glycerol; the use of dimethyl sulfoxide is associated, however, with much complication of the spectrum by matrix ions and adducts. Sulfolane proved to be the best matrix, giving good ion yields but virtually no adducts. The addition of dilute $HNO_3$ promoted the formation of low-mass clusters. A plot of $y$ *versus* $x$ gave an excellent straight line (41 points) of slope approximately 0.5, indicating that one additional O atom is incorporated for every two PrO units.

The CID spectra also feature odd–even alternation (Fig. 6); at low collision gas pressures the even-$x$ clusters disappeared

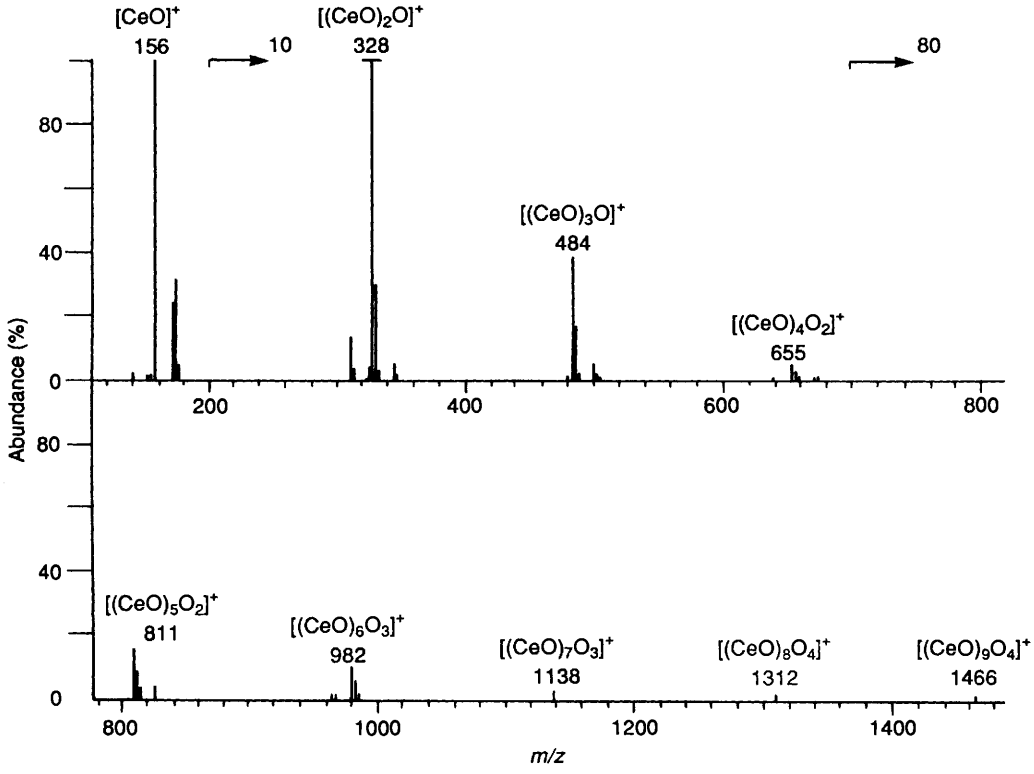


**Fig. 3** The FAB spectrum of cerium(IV) nitrate in a sulfolane matrix

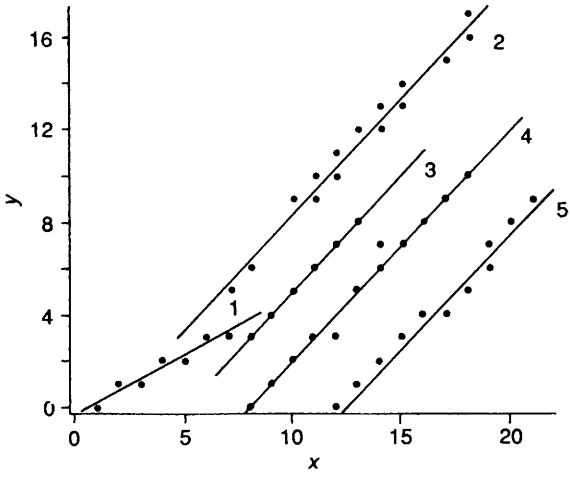


**Fig. 4** Variation of $y$ in $[(CeO)_xO_y]^+$ with cluster size $x$; the numbers refer to equations (9)–(12)

altogether. At higher pressures the odd-$x$ daughter clusters eliminate PrO units while even-$x$ daughters eliminate (PrO)O units.

Both the FAB and CID spectra indicate that the more elusive even-$x$ clusters require additional oxygen atoms to stabilise their structures.

*Samarium–Oxygen clusters.* The spectra were complicated by the presence of matrix adducts, and sulfolane proved to be the cleanest solvent from this point of view. A further complicating feature was the isotopic splitting associated with the seven natural isotopes of Sm. Species $[(SmO)_xO_y]^+$ were detected with $x$ up to 23. The base peak was $[SmO]^+$ and the abundances of higher clusters fell off as $x$ increased, although the peak due to $[(SmO)_9O_3]^+$ was unusually strong (Table 3).

*Europium–Oxygen clusters.* The presence of two isotopes in nearly equal abundance complicates the spectra of clusters at low mass, but at higher masses the statistical mixing leads to the situation of europium being best described by the averaged relative molecular mass. A range of matrices were employed and all gave the same basic series of clusters of general formula $[(EuO)_xO_y]^+$ (Fig. 7). The base peak was always $[EuO]^+$ although $[(EuO)O_4]^+$ was relatively abundant when a sulfolane matrix was used. The most abundant dieuropium species was $[(EuO)_2]^+$ while the dominant trieuropium species were $[(EuO)_3O]^+$ and $[(EuO)_3]^+$; other species in this series were $Eu_3^+$, $[Eu_2(EuO)]^+$ and $[Eu(EuO)_2]^+$. The most prominent members of the $x = 4$ series was $[(EuO)_4]^+$, while when $x = 5$, $y$ ranged from 0 to 2 with $y = 1$ and 2 dominant. The $x = 6$ series was dominated by $[(EuO)_6O_3]^+$. As $x$ increased further, $y$ also increased slowly but the smoothness of the trend was broken by the dominance of 'oxygen-deficient' peaks at $x = 4$, 9, 12, 15 and 20 (*i.e.* the most-abundant peak referred to one less oxygen than the value found for the preceding $x$ series). Abnormally intense peaks were located for $x$ values of 3, 10, 15 and 20, and in the range $x = 10$–20 there was evidence of even–odd alternation. In general terms, the FAB spectra of Eu–O clusters show behaviour quite unlike that of any other lanthanide examined.

The CID spectra for Eu–O clusters were rather irreproducible, with the incident-beam intensities proving stable over only a narrow range of sample conditions (temperature, matrix). The fragment-ion intensities were generally rather weak compared with those of other lanthanides; the range of $y$ values in each cluster series increased with increasing collision gas pressure, while lower values of $y$ were also associated with higher pressures. The fragmentation patterns (like the FAB spectra themselves) differed significantly from those found with oxygen clusters of La and Pr with the levels of 'additional' oxygen atoms being reduced rapidly upon each successive fragmentation. This usually occurred by the loss of (EuO)O units from both odd and even clusters to form species of general formula $[(EuO)_x]^+$. Generally clusters with odd values of $x$ showed a wider range of $y$ values, with $[(EuO)_5O_3]^+$ and $[(EuO)_3O]^+$ often detected in fragmentations, suggesting enhanced stability for these species.

*Terbium–Oxygen clusters.* Clusters of formula $[(TbO)_xO_y]^+$

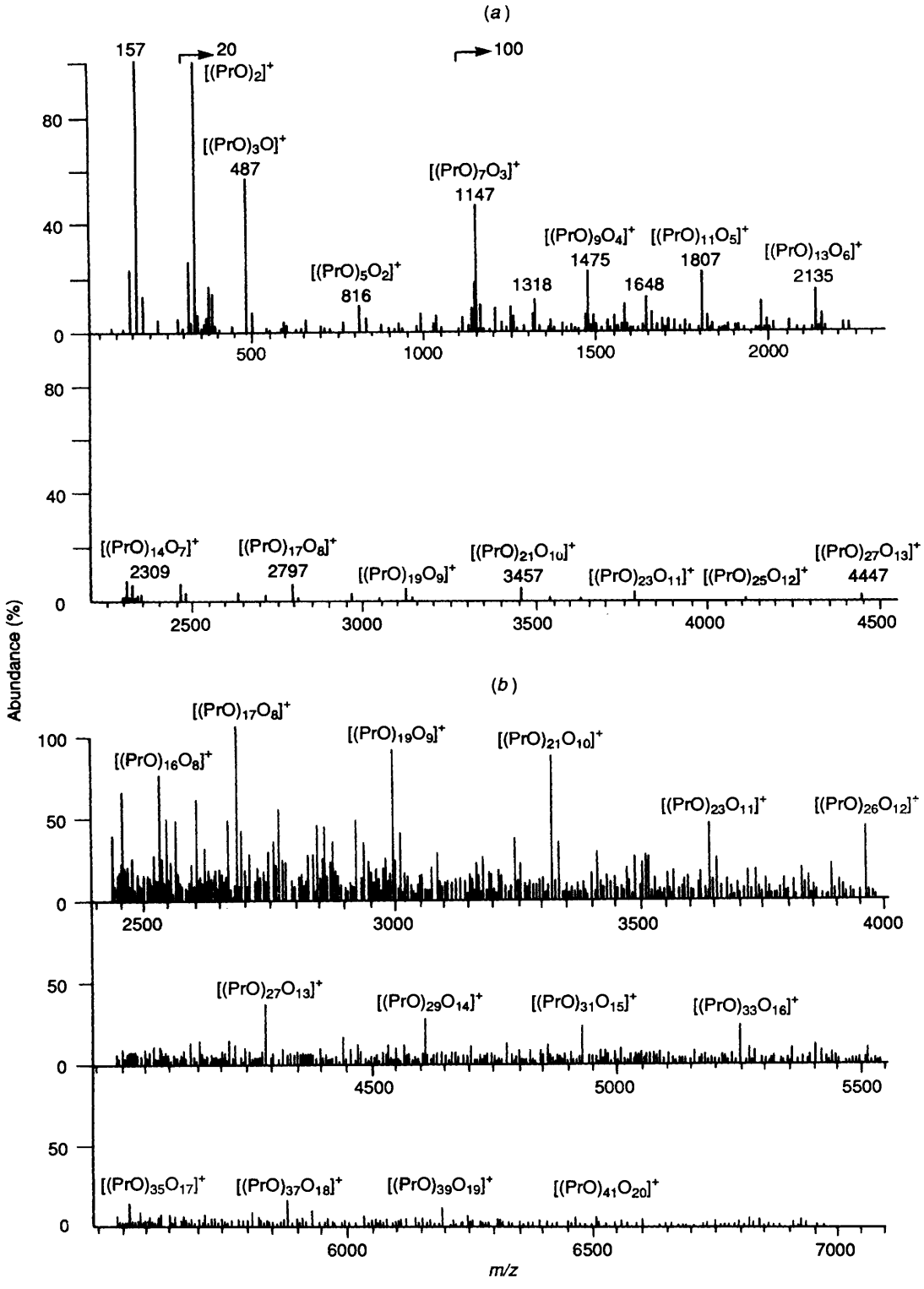


**Fig. 5** The FAB spectrum of praseodymium nitrate in sulfolane matrix: (*a*) mass range 1–4500; (*b*) mass range 2500–7000

were readily formed with all matrices. Table 3 shows the cluster abundances to fall off rapidly and exponentially with increasing cluster size and to display marked odd–even alternation (with relatively low abundance for even values of $x$). Plots of $y$ *versus* $x$ showed each successive even-$x$ cluster to accommodate one additional O atom. The pattern of take-up of additional O atoms resembled that found for Pr–O clusters.

*Holmium–oxygen clusters.* The FAB mass spectrum of holmium nitrate featured a series of clusters $[(HoO)_xO_y]^+$ extending to very high mass, *e.g.* $[(HoO)_{27}O_{14}]^+$ with $m/z$ 5085. There was a generally slow exponential reduction in abundance as $x$ increased, and even-$x$ clusters were of lower abundance than their odd-$x$ neighbours (Table 3).

For a given value of $x$ there was a limited range of $y$ values; each successive even-$x$ cluster was found to incorporate one additional O atom, *cf.* the situation with La–O clusters. There were perturbations to this sequence, however, with the co-ordination of three additional O atoms between $x = 19$ and 23. Again the abundance of the even-$x$ series drops sharply after the slightly increased abundance of the $[(HoO)_{22}O_{12}]^+$ cluster.

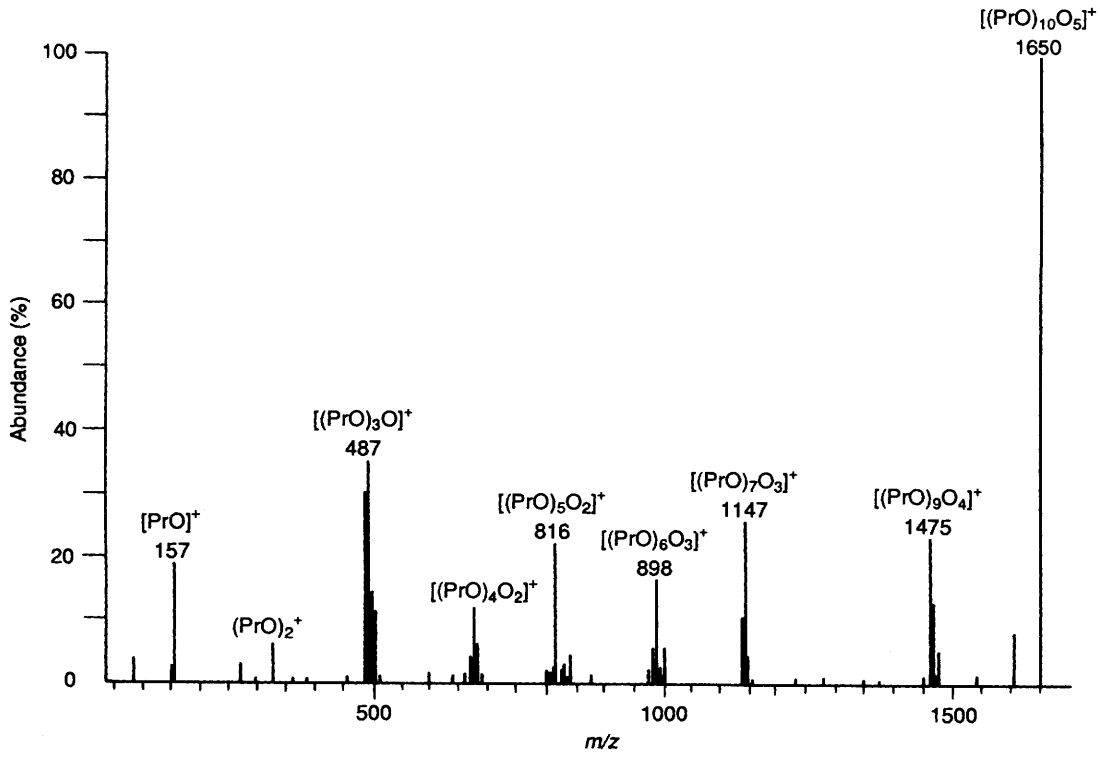


**Fig. 6** The CID spectrum of $[(PrO)_{10}O_5]^+$ ion

**Table 3** Metal oxide cluster ions in the FAB mass spectra of lanthanide salts in sulfolane matrices

| *m/z* (Relative abundance) | Species | *m/z* (Relative abundance) | Species |
|---|---|---|---|
| (*a*) Sm–O Clusters | | | |
| 169 (100) | $[SmO]^+$ | 1545 (2.14) | $[(SmO)_9O_5]^+$ |
| 339 (3.9) | $[(SmO)_2]^+$ | 1902 (0.49) | $[(SmO)_{11}O_4]^+$ |
| 517 (2.40) | $[(SmO)_3]^+$ | 2106 (1.91) | $[(SmO)_{12}O_7]^+$ |
| 851 (1.59) | $[(SmO)_5]^+$ | 2187 (0.34) | $[(SmO)_{13}O]^+$ |
| 1082 (2.66) | $[(SmO)_6O_5]^+$ | 2947 (0.03) | $[(SmO)_{17}O_8]^+$ |
| 1414 (1.18) | $[(SmO)_8O_5]^+$ | | |
| (*b*) Tb–O Clusters | | | |
| 175 (100) | $[TbO]^+$ | 906 (0.45) | $[(TbO)_5O_2]^+$ |
| 366 (5.0) | $[(TbO)_2O]^+$ | 1082 (0.09) | $[(TbO)_6O_2]^+$ |
| 541 (2.0) | $[(TbO)_3O]^+$ | 1273 (0.31) | $[(TbO)_7O_3]^+$ |
| 732 (0.39) | $[(TbO)_4O_2]^+$ | 1639 (0.10) | $[(TbO)_9O_4]^+$ |
| (*c*) Ho–O Clusters | | | |
| 180 (100) | $[HoO]^+$ | 2445 (0.38) | $[(HoO)_{13}O_6]^+$ |
| 378 (10.8) | $[(HoO)_2O]^+$ | 2633 (0.08) | $[(HoO)_{14}O_7]^+$ |
| 558 (7.3) | $[(HoO)_3O]^+$ | 2882 (0.16) | $[(HoO)_{15}O_7]^+$ |
| 756 (2.1) | $[(HoO)_4O_2]^+$ | 3200 (0.18) | $[(HoO)_{17}O_8]^+$ |
| 935 (2.5) | $[(HoO)_5O_2]^+$ | 3399 (0.08) | $[(HoO)_{18}O_{10}]^+$ |
| 1128 (2.1) | $[(HoO)_6O_3]^+$ | 3580 (0.18) | $[(HoO)_{19}O_{10}]^+$ |
| 1313 (2.35) | $[(HoO)_7O_3]^+$ | 3956 (0.11) | $[(HoO)_{21}O_{11}]^+$ |
| 1519 (2.5) | $[(HoO)_8O_4]^+$ | 4152 (0.04) | $[(HoO)_{22}O_{11}]^+$ |
| 1684 (0.56) | $[(HoO)_9O_4]^+$ | 4332 (0.10) | $[(HoO)_{23}O_{12}]^+$ |
| 1887 (0.22) | $[(HoO)_{10}O_5]^+$ | 4709 (0.04) | $[(HoO)_{25}O_{13}]^+$ |
| 2068 (0.52) | $[(HoO)_{11}O_5]^+$ | 5085 (0.03) | $[(HoO)_{27}O_{14}]^+$ |
| 2256 (0.21) | $[(HoO)_{12}O_6]^+$ | | |

After this discontinuity the value of $y$ increases uniformly, with the most-abundant member of each odd-$x$ series of clusters containing one additional O atom, *e.g.* as in $[(HoO)_{19}O_{10}]^+$, $[(HoO)_{21}O_{11}]^+$, $[(HoO)_{23}O_{12}]^+$, $[(HoO)_{25}O_{13}]^+$ and $[(HoO)_{27}O_{14}]^+$.

The CID spectra for Ho–O clusters showed these to undergo sequential loss of $(HoO)_2O$ units between odd clusters. Even-$x$ clusters were produced only under higher collision gas pressures, *cf.* the situation with CID of La–O and Pr–O clusters.

## Discussion

*Praseodymium- and Terbium–oxygen Clusters.*—The spectra

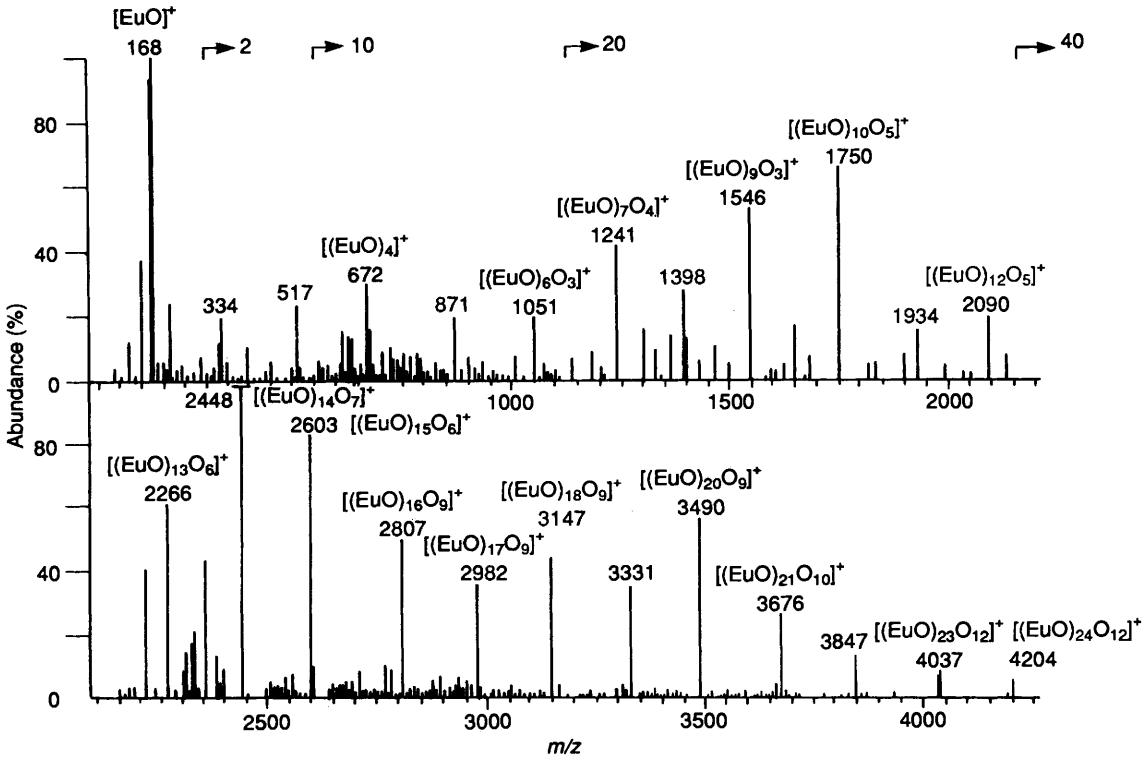


**Fig. 7** The FAB spectrum of europium nitrate in a sulfolane matrix

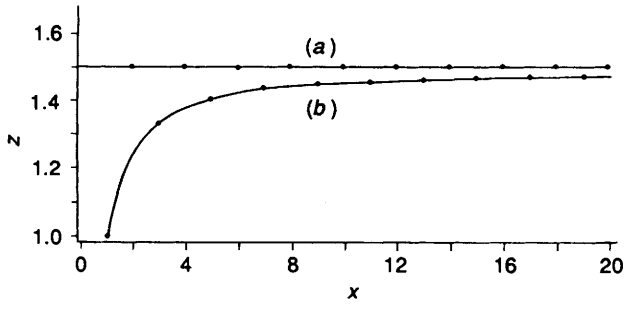


**Fig. 8** Variation of oxygen : metal ratio $z$ with cluster size $x$ for Pr–O and Tb–O cluster ions; (*a*) $x$ even, (*b*) $x$ odd

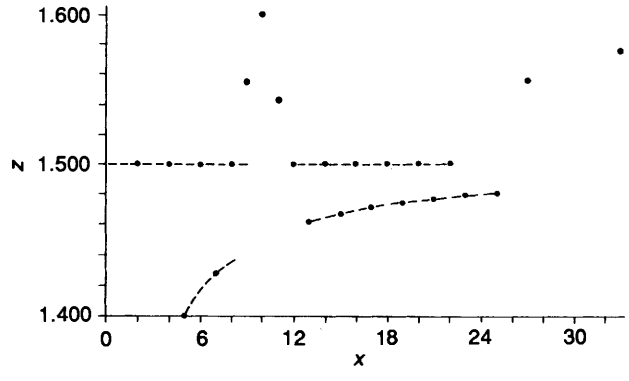


**Fig. 9** Variation of oxygen : metal ratio $z$ with cluster size $x$ for La–O cluster ions

obtained by FAB were relatively 'ideal' in that they displayed peaks of high abundance, with high reproducibility over a range of matrices. For these metals plots of $y$ *versus* $x$ gave two perfect, close and parallel straight lines, *i.e.* equation (5) for odd-$x$

$$y = 0.5x - 0.5 \quad (5)$$

clusters and (6) for even-$x$ clusters. A plot of total oxygen : metal

$$y = 0.5x \quad (6)$$

ratio ($= z$) *versus* $x$ (Fig. 8) reveals that even-$x$ clusters possess a stoichiometry of $[Ln_2O_3]^+$ for all values of $z$ whilst odd-$x$ clusters deviate strongly from this at low $x$ [tending obviously to a $[LnO]^+$ stoichiometry according to equation (5)], however at high values of $x$ the stoichiometry of the odd-$x$ clusters also tends to $[Ln_2O_3]^+$. A plot of $z$ *versus* $1/x$ is linear for the odd-$x$ clusters.

*Lanthanum–Oxygen Clusters.*—A plot of $y$ *versus* $x$ shows discontinuities in the regions of $x \approx 10$ and $> 25$, which are accentuated in a plot of the O : La ratio, $z$, *versus* $x$ (Fig. 9). With the exceptions of the discontinuities, even-$x$ clusters up to $x = 22$ give a uniform stoichiometry of 1.5, *i.e.* the cluster is $[(La_2O_3)_{x/2}]^+$ while odd-$x$ clusters show a trend to increase from a starting point of $[LaO]^+$ towards an O : La ratio of 1.5 : 1 (*e.g.* 1.480 at $x = 25$). The species $[(LaO)_{10}O_6]^+$ with O : La = 1.60 : 1 which is flanked by lanthanum-rich $La_9$- and $La_{11}$-based clusters, represents a clear change in structure at a particular point, presumably associated with a special level of stabilisation.

*Holmium–Oxygen Clusters.*—Discontinuities in stoichiometry are also a prominent feature in Ho–O cluster ions. A plot of $y$ *versus* $x$ yields two parallel straight lines of slope 0.5 but with a clear break at $x = 20$. This is highlighted in a plot of the ratio O : Ho *versus* $1/x$ shown in Fig. 10, which features three lines all converging asymptotically to O : Ho = 1.5 : 1, *i.e.* $[(Ho_2O_3)_{x/2}]^+$. The data for even-$x$ clusters show unvarying stoichiometry of O : Ho = 1.5 : 1 throughout, but stop abruptly at $x = 18$ above which no even-$x$ clusters are detected. For odd-$x$ clusters with $x \leqslant 19$ the O : Ho ratio increases in a manner similar to those observed for Pr–O and Tb–O clusters, but at $x \geqslant 21$ the O : Ho ratio increases abruptly to a figure exceeding 1.5 : 1 before decreasing thereafter towards the 'ideal' ratio of 1.5 : 1. The two linear plots for the odd-$x$ clusters can be

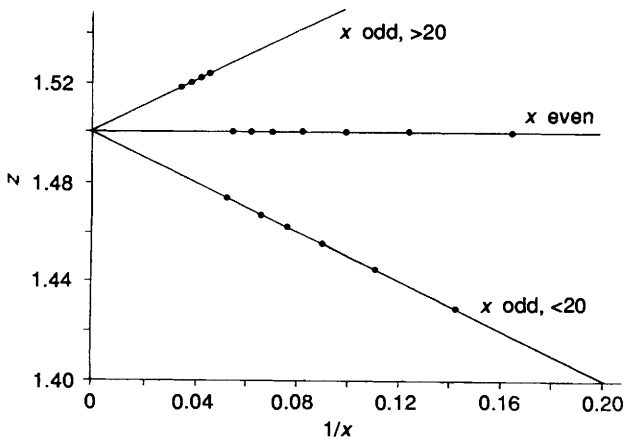


**Fig. 10** Variation of oxygen : metal ratio $z$ with reciprocal cluster size $1/x$ for Ho–O cluster ions

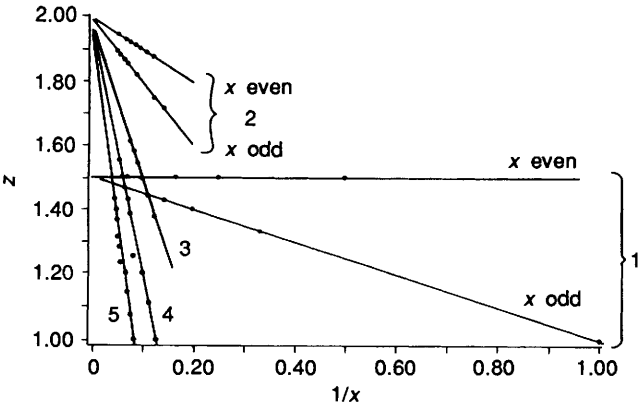


**Fig. 11** Variation of oxygen : metal ratio $z$ with reciprocal cluster size $1/x$ for Ce–O cluster ions [numbers refer to series of ions 1–5; see text and equations (9)–(12)]

represented by equations (7) and (8). This change in stoichiometry at $x = 20$ is considered to be related to the adoption of a different internal structure by the clusters.

$$x \leqslant 19, \quad O:Ho = (-0.5/x) + 1.5 \qquad (7)$$

$$x \geqslant 21, \quad O:Ho = (0.47/x) + 1.5 \qquad (8)$$

*Cerium–Oxygen Clusters.*—The stoichiometries of Ce–O clusters change with increasing cluster size in a manner quite distinct from those of the other lanthanides examined. A plot of $y$ *versus* $x$ (Fig. 4) shows, for small clusters ($x \leqslant 8$), behaviour like other lanthanides (Line 1). Once $x$ exceeds 8 the stoichiometries of the most abundant clusters in the series $[(CeO)_xO_y]^+$ fall into *four* groups, indicated by the straight lines numbered 2–5 in Fig. 4. These lines can be represented by equations (9)–(12).

Line 2 $\quad y = x - 1 \qquad (9)$

Line 3 $\quad y = x - 5 \qquad (10)$

Line 4 $\quad y = x - 8 \qquad (11)$

Line 5 $\quad y = x - 12 \qquad (12)$

A plot of O : Ce *versus* $1/x$ (Fig. 11) shows two trends: (*i*) At low $x$ values even-$x$ clusters all show a stoichiometry of 1.5 while odd-$x$ clusters deviate from this figure but approach it as

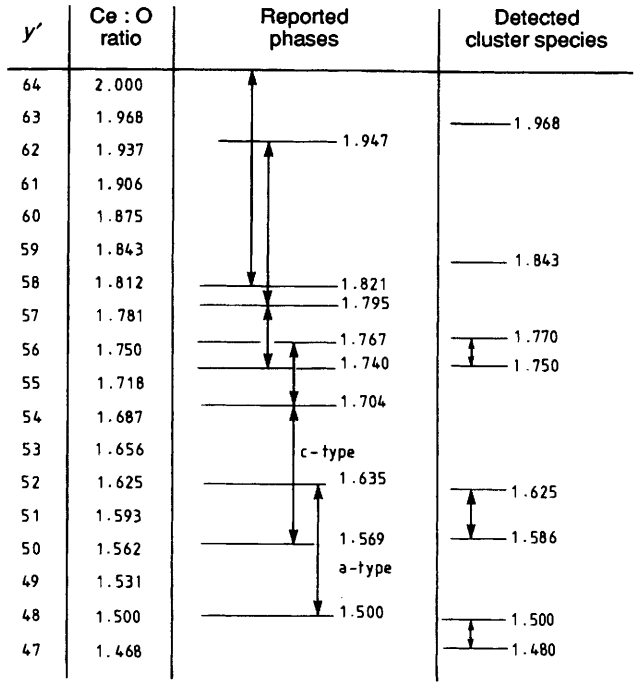


**Fig. 12** Comparison of stable Ce–O stoichiometries in the solid phases $Ce_{32}O_{y'}$ and gas-phase $[(CeO)_xO_y]^+$ cluster ions of $Ce_{32}O_{y'}$

**Table 4** Ratios O : Ce in the bulk phase and in Ce–O positive-ion clusters

| Cluster series in Fig. 11 | O : Ce ratio | | Structure in bulk phase |
|---|---|---|---|
| | In cluster | In bulk phase | |
| 2 | 1.968 | 1.821–2.99 (α) | Face-centred cubic |
| 3 | 1.843 | 1.792–1.947 (β) | Rhombic |
| 4 | 1.75–1.77 | 1.740–1.785 (γ) | Rhombic |
| 5 | 1.57–1.63 | 1.569–1.704 (c type) | Body-centred cubic |

$x$ increases; (*ii*) at $x > 10$ the stoichiometries of the series 2–5 (Fig. 4) all converge towards an ultimate value at infinite $x$ of 2.0, *i.e.* the oxidation state +4 in $CeO_2$. For series 2 the stoichiometries of the even-$x$ and odd-$x$ series are differentiated, the former being nearer to 2.06 throughout. The range of stoichiometries found in the Ce–O clusters recalls that described for Ce–O phases in the bulk by Bevan.[10] Fig. 12 shows the comparison clearly, and Table 4 illustrates this further.

Accordingly, it seems that the set of Ce–O cluster stoichiometries evident in Fig. 12 may refer to the adoption of different lattice structures within the cluster corresponding to those defined for the bulk solid material. The adoption of well defined structures in gas-phase species which reproduce those of proven existence in the solid state is well known, not least for $C_{60}$.

*Europium–Oxygen Clusters.*—The picture here was one of some complexity, with rather few of the recognisably simplifying trends described above for lanthanide–oxygen clusters (Ln = La, Ce, Ho, Pr or Tb). The plot of cluster abundance *versus* cluster size [Fig. 13(*a*)] gave a series of discontinuities, with larger-than-expected abundances at $x = 3$, 7, 10, 14 and 20. A plot of $y$ *versus* $x$ gave, instead of the normal straight line, a series of discontinuities about an overall upward trend [Fig. 13(*b*)], with sudden drops in $y$ at $x = 4$, 9, 15 and 20 [*i.e.* near the discontinuities in Fig. 13(*a*)]. The near-coincidence of the appearance of the discontinuities points to an underlying effect,

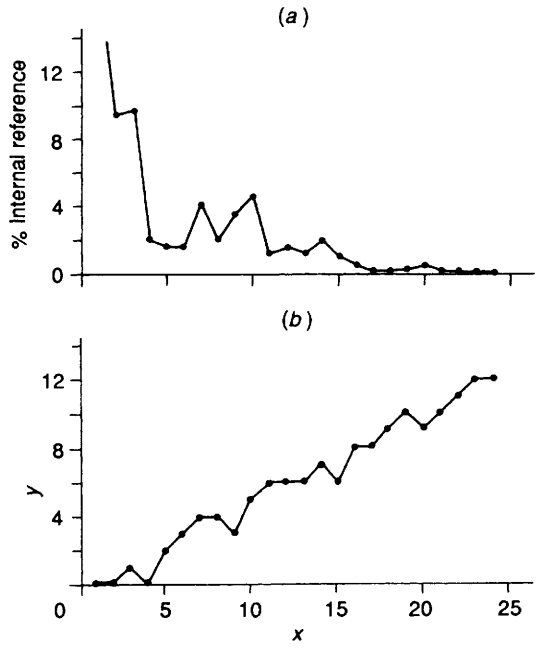


**Fig. 13** Variation in (*a*) relative abundance and (*b*) value of $y$ with increasing cluster size $x$ for Eu–O cluster ions

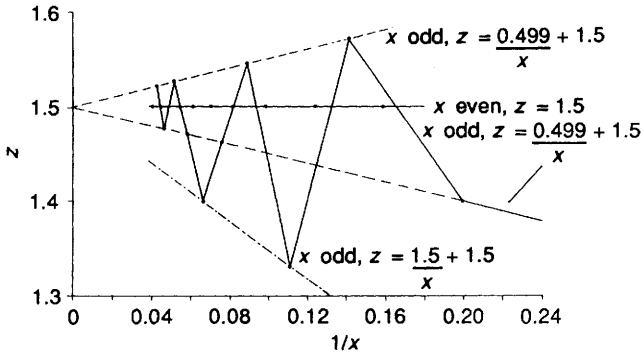


**Fig. 14** Variation of oxygen:metal ratio $z$ with reciprocal cluster size $1/x$ for Eu–O cluster ions

presumably the emergence of structures of enhanced stability. A plot of the O:Eu ratio *versus* $1/x$ (Fig. 14) is remarkable even in the intriguing lanthanide–oxygen catalogue. As we often find, the even-$x$ clusters all show a stoichiometry of 1.5 for O:Eu, *i.e.* they refer to clusters $[\{(EuO)_2O\}_x]^+$. The odd-$x$ clusters fall on three lines and the stoichiometry oscillates between these, ultimately converging towards O:Eu = 1.5:1. The equations of the lines connecting members of the series are (13)–(15). The

$x \leqslant 5$ O:Eu = 1.5 − (0.5/$x$) (13)

$x \geqslant 7$

(*a*) $x$ given by 5 + 4$n$ ($n$ = 1, 2, *etc.*): (13) above

(*b*) $x$ given by 7 + 4$n$

O:Eu = 1.5 + (0.5/$x$) (14)

(*c*) (exceptions) $x$ = 9 or 15

O:Eu = 1.5 − (1.5/$x$) (15)

two exceptions refer, in fact, to the two most-abundant species in the FAB spectrum.

*Samarium–Oxygen Clusters.*—A plot of $y$ *versus* $x$ for $x \leqslant 23$ for the most-abundant Sm–O clusters give rise to a series of

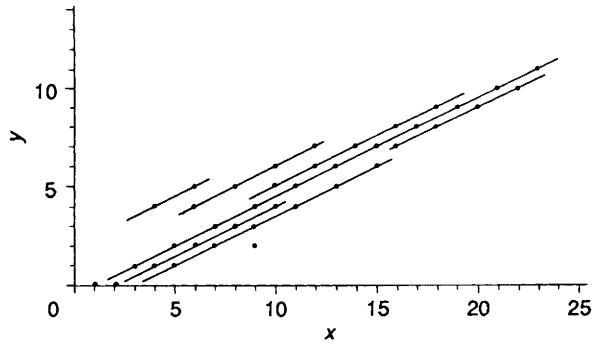


**Fig. 15** Variation of $y$ in samarium–oxygen cluster ions $[(SmO)_xO_y]^+$ with cluster size $x$

distinct linear regions for both odd and even values of $x$ (Fig. 15). The odd-$x$ clusters followed equation (5) over the full range of $x$, with an additional dependence (16) being found

$$y = 0.5x - 1.5 \quad (16)$$

for $5 \leqslant x \leqslant 15$. For even-$x$ clusters the picture is more complex: at $x \leqslant 10$ and 16–22 equation (17) holds, whereas

$$y = 0.5x - 1.0 \quad (17)$$

when $x$ = 12 or 14 equation (6) holds. Evidence also was found for the coexistence of a series of even-$x$ clusters of higher oxygen content, *viz.* equations (18) and (19).

$x = 4, 6$ $y = 0.5x + 2.0$ (18)

$6 \leqslant x \leqslant 12$ $y = 0.5x + 1.0$ (19)

Plots of the O:Sm ratio *versus* $x$ showed all observed cluster stoichiometries to lie on one of six lines radiating from O:Sm = 1.5:1 at $x = \infty$ (Fig. 16), *i.e.* all families of clusters tend to a stoichiometry $(Sm_2O_3)_{x/2}$ at high values of $x$, while exhibiting strong positive or negative deviations from this for small clusters. Sharp changes occur in the O:Sm ratio near $x$ = 6, 10, 15 and 19 (*cf.* the comparable figures for europium–oxygen clusters of 4, 9, 15 and 20, Fig. 13). This similarity in behaviour between Eu and Sm is undoubtedly related to their abilities to adopt the +2 as well as the +3 oxidation state.

*General Comment.*—While each set of lanthanum–oxygen cluster ions shows distinctive, sometimes rather complex, behaviour, there are points in common. Thus all the series exhibit a stoichiometry $[(LnO)_2O]_{x/2}$ over part of the range of $x$ values, or sometimes over the complete range for even values of $x$.

The cluster spectrum for most lanthanides where $x$ is an odd number can be expressed by equation (20) (with the negative

$$z = (\pm 0.5/x) + 1.5 \quad (20)$$

quadrant being dominant). A number of lanthanides (Eu, Sm, La and Ho) show discontinuities in the abundance *vs.* $x$ plots near $x$ = 10, 15 and 20, which coincide with abrupt changes in $z$; both Eu and Sm exhibit odd-$x$ clusters corresponding to the relationship (21) which reflects their ability to adopt an

$$z = (-1.5/x) + 1.5 \quad (21)$$

oxidation state of +2.

The ready accessibility of the +4 oxidation state to Ce accounts for the high O:Ce stoichiometry observed in some Ce–O cluster ions (Fig. 11).

The odd–even alternation effects in both FAB and CID

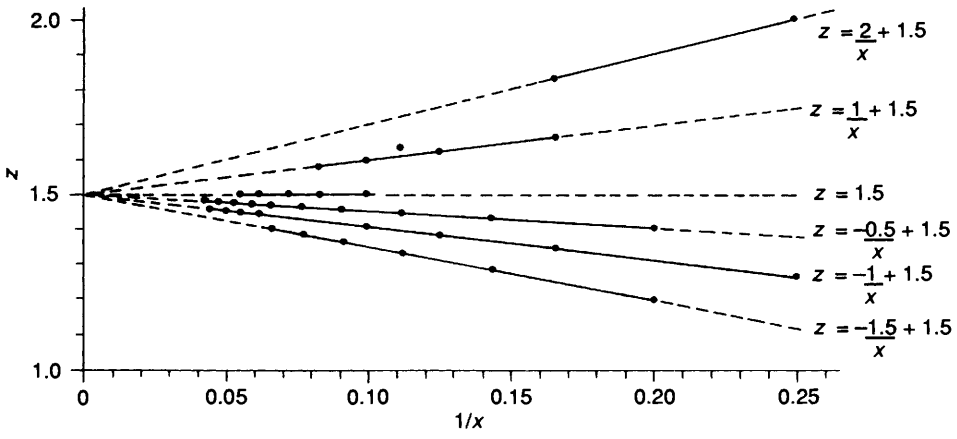


**Fig. 16** Variation of oxygen : metal ratio $z$ with reciprocal cluster size $1/x$ for Sm–O cluster ions

spectra can be explained in terms of electron counts: an even-$x$ cluster will be associated with $1.5x$ oxygen atoms, *i.e.* an even number; there will be no unshared electrons and ionisation involves generating a relatively energetic paramagnetic species. An odd-$x$ cluster will be associated with a number of oxygen atoms other than that required to achieve a metal oxidation state of exactly +3, thus the pentalanthanum cluster will either be $[(LnO)_5O_2]$ or $[(LnO)_5O_3]$ which are paramagnetic: ionisation of these will be relatively thermodynamically favoured to give the diamagnetic $[(LnO)_5O_2]^+$ and $[(LnO)_5O_3]^+$ respectively.

## Acknowledgements

We thank the SERC for a studentship (to P. A. R.) and Professor K. R. Jennings and his group for assistance in conducting the experiments.

## References

1 M. I. Bruce and M. J. Liddell, *Appl. Organomet. Chem.*, 1987, **1**, 191.
2 M. Barber, R. S. Bordoli, R. D. Sedgwick and A. N. Tyler, *J. Chem. Soc., Chem. Commun.*, 1981, 325.
3 T. J. Kemp, K. R. Jennings and P. A. Read, *J. Chem. Soc., Dalton Trans.*, following paper.
4 I. A. Kahwa, J. Selbin, T. C.-Y. Hsieh and R. A. Laine, *Inorg. Chim. Acta.*, 1988, **141**, 131.
5 I. A. Kahwa, J. Selbin, T. C.-Y. Hsieh, D. W. Evans, K. M. Pamidimukkala and R. Laine, *Inorg. Chim. Acta*, 1988, **144**, 275.
6 W. Yu and R. B. Freas, 36th American Society for Mass Spectrometry Conference, San Francisco, 1988.
7 R. L. Whetten, D. M. Cox, D. J. Trevor and A. Kaldor, *J. Phys. Chem.*, 1985, **89**, 566.
8 J. M. Curtis, P. J. Derrick, A. Schnell, E. Constantin, R. T. Gallagher and J. R. Chapman, *Inorg. Chim. Acta*, 1992, **201**, 197.
9 J. M. Curtis, P. J. Derrick, A. Schnell, E. Constantin, R. T. Gallagher and J. R. Chapman, *Org. Mass Spectrom*, 1992, **27**, 1176.
10 D. J. M. Bevan, *J. Inorg. Nucl. Chem.*, 1955, **1**, 49.

*Received 9th June* 1994; *Paper* 4/03481C